C. R. Biologies 325 (2002) 917–925

S163106910201507X/FLA

Hypotheses and modelling / Hypothèses et modélisation

Quasi-periodic behaviour in a model for the lithium-induced, electrical oscillations of frog skin

Christophe Letellier[a], Jean-Paul Lassalles[b], Vic Norris[c], Camille Ripoll[c], Michel Thellier[c]*

[a] *CORIA, université de Rouen, av. de l'Université, BP 12, 76801 Saint-Étienne-du-Rouvray cedex, France*

[b] *Laboratoire des processus ioniques membranaires, faculté des Sciences, université de Rouen, place Émile-Blondel, 76821 Mont-Saint-Aignan cedex, France*

[c] *Laboratoire des processus intégratifs cellulaires, faculté des Sciences, université de Rouen, place Émile-Blondel, 76821 Mont-Saint-Aignan cedex, France*

Received 18 February 2002; accepted 30 July 2002

Presented by Michel Thellier

Abstract – The fact that oscillations can be induced in studies of the maintenance of the electrical potential of frog skin by addition of lithium allowed evaluation of several parameters fundamental to the functioning of the system in vivo (e.g. relative volumes of internal compartments, characteristic times of ionic exchanges between compartments). A realistic model was thus proposed under the form of a set of ordinary differential equations. In the past, numerical simulations using such a model reproduced the periodic experimental oscillations and was able to provide an explanation for the global synchronised oscillations of the whole skin. In that paper, new numerical simulations reproduce the non-periodic oscillations which were observed two decades ago, but not reproduced by the model. Moreover, the dynamical process under which all the local oscillators are synchronised is explained in terms of a tangent bifurcation. ***To cite this article: C. Letellier et al., C. R. Biologies 325 (2002) 917–925.*** © 2002 Académie des sciences / Éditions scientifiques et médicales Elsevier SAS

electric oscillations / quasi-periodic behaviour / nonlinear dynamics

Résumé – Comportements quasi-périodiques dans un modèle des oscillations électriques induites par le lithium de peaux de grenouilles. Le fait que des oscillations puissent être induites dans l'étude du maintien du potentiel électrique de peaux de grenouilles par ajout de lithium a permis l'évaluation de plusieurs paramètres fondamentaux liés au fonctionnement du système in vivo (par exemple, les volumes relatifs des compartiments internes, les temps caractéristiques des échanges ioniques entre compartiments). Un modèle réaliste fut ainsi proposé sous la forme d'un système d'équations différentielles ordinaires. Par le passé, des simulations numériques utilisant un tel modèle reproduisaient les oscillations périodiques expérimentales et permettaient de fournir une explication pour la synchronisation globale de l'ensemble de la peau. Dans cette note, de nouvelles simulations numériques reproduisent les oscillations non périodiques qui furent observées il y a une vingtaine d'années, mais alors non reproduites par le modèle. De plus, le mécanisme dynamique par lequel tous les oscillateurs locaux sont synchronisés est expliqué en termes de bifurcation tangente. ***Pour citer cet article : C. Letellier et al., C. R. Biologies 325 (2002) 917–925.*** © 2002 Académie des sciences / Éditions scientifiques et médicales Elsevier SAS

oscillations électriques / comportement quasi périodique / dynamique non linéaire

*Correspondence and reprints.
E-mail address: Michel.Thellier@univ-rouen.fr (M. Thellier).

1. Introduction

Frogs maintain the saline concentration of their internal medium, even when immersed in a diluted external medium, such as a fresh water pond, due to the activity of a Mg-dependent Na–K–ATPase that creates a steady transepithelial potential difference in the range of a few tens to more than a hundred mV (positive inside). This active ion-pumping system has been studied in great detail, especially by Ussing's group [1,2], using the ventral skin of frogs mounted between two aqueous chambers filled with appropriate saline solutions. However, although, for the sake of experimental commodity, most experiments have been carried out by Ussing and followers using samples of the whole skin, it is only the epithelium layer of the skin that controls the ion exchanges and the maintaining of the electric potential difference of the skin [3]. Maintaining the electrical potential of frog skin under these conditions requires sodium in the external medium. Lithium is the only ion that can be used instead [4]. However, when all or part of the external sodium is replaced by lithium, the electric potential frequently oscillates [5–7], which it never does in the absence of lithium (Fig. 1). Our group has been particularly involved in the understanding of the generation of such oscillations, from both experimental and theoretical points of view [7–11]. As it will be explained in section 3, a set of two ordinary differential equations were obtained to describe the dynamics of a fragment of the skin. It generates periodic oscillations. In section 4, the case of oscillations for which the amplitude fluctuates (Fig. 1b) is investigated. Section 5 gives a conclusion.

2. Local nature of the oscillator

The first question to be addressed was to determine whether the oscillation has a local character (that is, if it exists at the level of each individual cell or of a small group of cells of the epithelium) or if it is a property of the entire fragment of skin under study. It was technically impossible to carry out an experimental study of the oscillation at the level of a single cell or of a very small group of cells; but when studying three skin fragments, taken from the same frog skin, whose areas where 0.28, 0.8 and 2 cm^2, in five successive experiments, the periods of oscillation (min) were found to be (mean ± confidence interval) 6.1 ± 1.4, 6.0 ± 0.9 and 6.3 ± 1.0, respectively, which means that the period of oscillation does not depend significantly on the area of

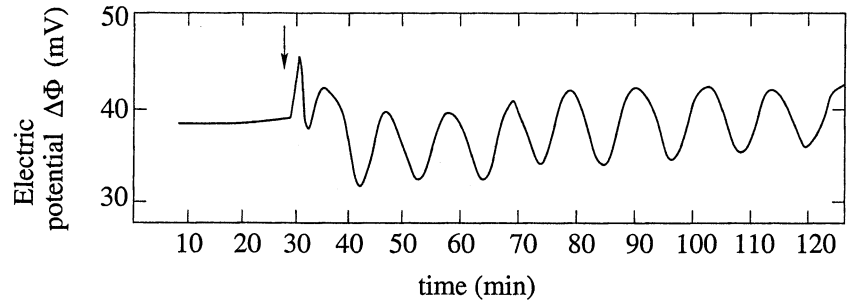

(a) Periodic oscillations

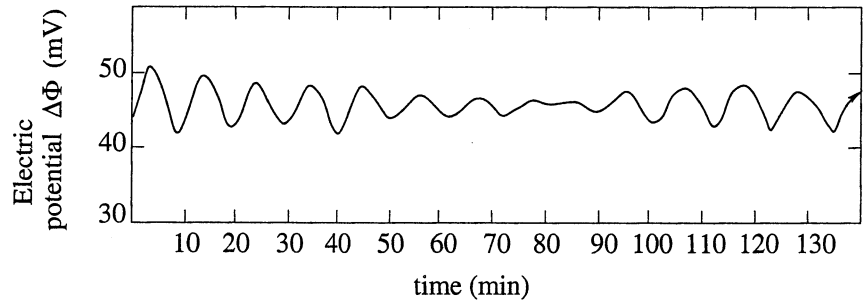

(b) Aperiodic oscillations

Fig. 1. Oscillations of the transepithelial electric potential $\Delta\phi$ (in mV and relative to external medium). (**a**) Initiation of the oscillation and its stability with time. At the time indicated by the arrow, the external Ringer solution was changed for a 115 mM LiCl solution: oscillations started almost immediately, and were sustained during several hours. (**b**) A complex type of behaviour was sometimes observed. The oscillations seems to vanish spontaneously and start again. The shape of the oscillation curve suggests the occurrence of an interference between several individual oscillatory processes. Adapted from [9].

skin under study [9]. In another series of experiments, using subcompartmentalised chambers, it has been possible to study simultaneously different parts of a single skin subjected to identical ionic conditions [9]. It turned out that the different parts of the skin exhibited oscillations of their electric potential difference, but these oscillations were out of phase with each other; moreover, the amplitude of these oscillations and the time during which each of them was sustained varied from one zone of the skin to another. These findings, plus the fact that the processes involved in the maintaining of the skin potential (ion pumping and passive transmembrane ion diffusion) exist at the cellular level, suggest that the skin behaves as a 'mosaic' of local oscillators (each oscillating in its own way or perhaps not oscillating at all). This, however, raises the problem of understanding how all the local oscillators are synchronised with one another in order to produce a visible electric oscillation of the whole skin fragment under consideration.

Interpreting the oscillation of the electric potential of the frog skin thus has to be addressed in two steps: (*i*) functioning of the local oscillator and (*ii*) synchronisation of local oscillators.

3. Characterisation of the local oscillator

3.1. Summarising the experimental observations

Our group [7,9] has shown experimentally that (*i*) when no transepithelial potential is imposed, sustained oscillations with a period of about 10 min are maintained for several hours, (*ii*) an oscillation of the Na^+ influx accompanies the electric oscillation (the two oscillations have approximately the same period but are not in phase), (*iii*) under conditions of imposed potential the transepithelial electric current has damped oscillations, (*iv*) the shape of the oscillations in potential is quite variable (from almost sinusoidal to very complex), (*v*) theophyllin (which induces an accumulation of cyclic AMP within the cells) promotes a significant decrease in the mean electric potential of the skin, but does not affect the characteristics of the oscillation very much, (*vi*) the osmotic pressure has little effect on the oscillation and (*vii*) important factors influencing the oscillations include temperature, the permeability of the external membrane to lithium and the potassium concentration in the internal medium.

3.2. Modelling the epithelium

A body of evidence obtained by others and cited in Lassalles et al. [10] demonstrates that the epithelium separating the external, E, and internal, I, solutions may

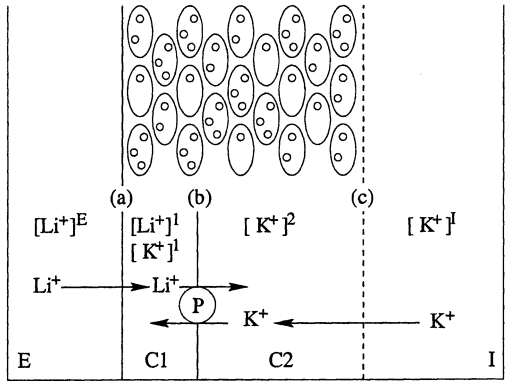

Fig. 2. Modelling frog skin epithelium. Top: schematic representation of the cellular structure of frog skin epithelium, mounted between two aqueous, saline solutions, E and I. Bottom: the epithelium model for ionic exchanges. The frog epithelium is modelled as corresponding to two compartments C_1 and C_2 with three barriers, (**a**) between E and C_1, (**b**) between C_1 and C_2 and (**c**) between C_2 and *I*. Symbol $[x]^j$ stands for concentration of cation *x* in compartment *j*. The Na–K–ATPase, P, pumps actively Li^+ from C_1 to C_2 and K^+ from C_2 to C_1.

be modelled as follows (Fig. 2). It is made of a few cell layers with two main cellular compartments, C_1 and C_2. The membrane, (**a**) is relatively permeable to Na^+ and Li^+ at the external face of the epithelium, whilst it is almost impermeable to K^+. The membrane, (**b**), between compartments C_1 and C_2 is permeable to K^+, but not to Na^+, and contains the Na–K–ATPase, pumping sodium and (less efficiently) lithium from C_1 to C_2 and pumping potassium from C_2 to C_1. When this active pump is fully efficient (Na^+ pumping in the absence of any inhibitor), the first cellular layer is enough to pump out practically all of the Na^+, but, when it is not fully efficient (Li^+ pumping or Na^+ pumping in the presence of an inhibitor), the remaining ions diffuse to the other cell layers, which will therefore contribute to their active extrusion; as a consequence, it is likely that the overall transepithelial flux densities obtained for Li^+ and Na^+ are not too different from each other. The face, (**c**), between epithelium and internal medium is not an actual membrane, but may be considered rather as a non-selective diffusive barrier.

3.3. The local-oscillator model

Combining the experimental observations relative to the electric oscillations of the frog skin (section 3.1) with the epithelium model (section 3.2), it appears [8,10] that the set of variables involved in the system under study may be reduced to the following set of main variables: the concentration of Li^+ in compartment C_1, $[Li^+]^1$, and that of K^+ in compartment C_2, $[K^+]^2$, the characteristic times, τ_1 and τ_2, defined as

corresponding to variations of the Li^+ concentration in C_1 and variations of the K^+ concentration in C_2, the volumes v_1 and v_2 of compartments C_1 and C_2 per unit surface of epithelium, some permeability coefficients, P_K^b, P_K^c and P_{Li}^a, of the interfaces (a, b or c) for the ions K^+ and Li^+, and two parameters, ρ and μ, representing the relative importance of the active to the passive fluxes of Li^+ and K^+, respectively.

After a normalisation of the variables [8], a set of two ordinary differential equations is obtained:

$$\begin{cases} \dot{x} = 1 - x - \rho\, y\, \theta(x) + K_c \\ \dot{y} = \alpha\, [\, 1 - y - \mu\, y\, \theta(x)\,] \end{cases} \qquad (1)$$

where x and y are the normalised concentrations of Li^+ in C_1 and of K^+ in C_2. The parameter α is equal to τ_1/τ_2 The constant K_c designates the influence of a possible external current. Lithium is a substrate for the pump, but it is assumed to inhibit it at high concentration [8] (the so-called 'substrate inhibition' effect). Therefore, lithium action may be represented by the function $\theta(x)$, which takes the form

$$\theta(x) = \frac{x}{1 + \beta\, x + K\, x^3} \frac{1 + \beta\, x_m + K\, x_m^3}{x_m} \qquad (2)$$

where x_m designate the value of x at which $\theta(x) = 1$. Such a form of $\theta(x)$ is responsible for equations (1) being non-linear. Control parameters β and K determine the shape of the function. For plausible values of the different control parameters [10], the model (1) generates a limit cycle, i.e. sustained periodic oscillations (Fig. 3). It is therefore possible to reproduce qualitatively the experimental oscillations as shown in Fig. 1a.

It proved impossible [10] to adjust the numerical simulations (Fig. 3) to the observed characteristics (Fig. 1a) of the oscillatory process, unless the model

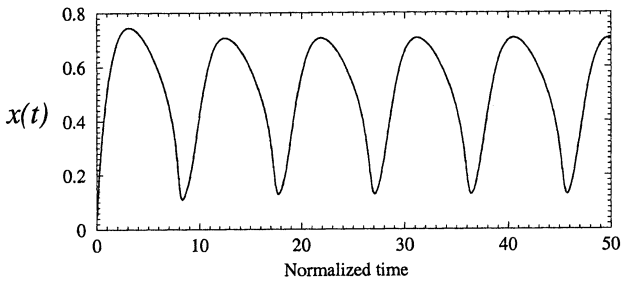

Fig. 3. Sustained periodic oscillations generated by the local model for the epithelium of a frog skin under effect of lithium ($\alpha = 0.2$, $\rho = 8.0$, $\mu = 10.0$, $\beta = 5.0$, $x_m = 0.14$ and $K_c = 0.1$).

had the following well-defined properties. v_1 and v_2, the volumes of compartments C_1 and C_2 per unit surface of epithelium, obey the relation $v_1/v_2 \ll 1$, i.e. compartment C_2 has to be much larger than compartment C_1. Two conflicting hypotheses (cited in Lassalles et al. [10]) have been proposed in the literature with regard to the exact nature of compartments C_1 and C_2. According to the first hypothesis, C_1 corresponds to most of the cytoplasmic volume and C_2 is restricted to a few endoplasmic cisternae (i.e. C_2 is much smaller than C_1). According to the second hypothesis, compartment C_1 corresponds to a few cytoplasmic vacuoles transporting Na^+ (and Li^+) and compartment C_2 is part or all of the intercellular spaces and possibly some endoplasmic cisternae (i.e. C_2 is much larger than C_1). Our finding that an oscillatory behaviour can be met only when $C_2/C_1 \geqslant 1$ thus supports the second hypothesis, while it rules out the first one, which also means that most of the cell cytoplasm would remain inactive in Na^+ (or Li^+) transport. The ratio of the characteristic times, τ_1 and τ_2 (corresponding to Li^+ modifications in C_1 and K^+ modifications in C_2) obeys the relation $0 < \tau_1/\tau_2 < 1$ with $1\ \text{min} \leqslant \tau_1 \leqslant 5\ \text{min}$. The parameters, ρ and μ, representing the relative importance of the active to the passive fluxes of Li^+ and K^+, respectively, must be such that $\rho \gg 1$ and $\mu \gg 1$, with $\rho \leqslant \mu \leqslant 2\,\rho$ (i.e. ρ and μ are of the same order of magnitude) in order to have oscillations. For similar reasons, the permeability coefficients of interfaces **a**, **b** and **c** for ions K^+ and Li^+ must be such that $P_k^b/P_K^c \ll 1$ and $P_{Li}^a/P_K^c \ll 1$. These conditions have been identified from the model.

4. Synchronisation of the local oscillations

4.1. Summarising the experimental study

In a number of experiments [8,9], a frog skin was divided into two parts, each mounted between two chambers containing the same internal medium (Ringer solution) and the same external medium (LiCl solution), in order to induce oscillations of the electric potential difference. Electrical bridges were prepared by filling plastic catheters with a gelose gel enriched with mineral salts, their electric resistance, R_c, depending on the saline concentration of the gel. When a single bridge was used (either between the two internal or between the two external solutions), synchronisation never occurred; the two skin fragments continued oscillating independently from each other. When two bridges were used, for connecting the internal solutions with each other on the one hand and the external

solutions with each other on the other hand, and when these bridges were with a relatively low electric resistance ($\leqslant 1\text{k}\Omega$) synchronisation occurred almost immediately. When the electric resistance of the bridges was increased up to several kΩ, the two epithelium fragments again oscillated independently from each other. Moreover, when an electric current was imposed to an oscillating epithelium, using an external electrical source, this tended to damp the oscillation. These data render it very unlikely that synchronisation may be due to a diffusion–reaction process, but they are very consistent with the occurrence of electrical coupling.

4.2. Theoretical interpretation and numerical simulations

Electric potentials pass mainly through internal and external electrolytes. They induce fluctuations of the concentration within the cells [8]. The epithelium is thus considered like a huge cell with a potential φ that tends to drive the current in the cell j, with a lithium concentration x_j, a potential φ_j and a current I_j. This current induces an additional diffusion flux of lithium through the membrane. In the first equation of the local model (1), a diffusion term within the cell, $1 - x_j$, is thus added. The term $\delta \log \frac{U}{x_j}$, where $U = \sum_{j=1}^{n} x_j$ is the averaged concentration over all the cells, designates the electrical coupling between the epithelium fragments.

The model for n cells thus reads as

$$\begin{cases} \dot{x}_j = 1 - x_j - \rho\, y_j\, \theta(x) + K_c + \delta \log\left(\dfrac{U}{x_j}\right) \\ \qquad\qquad\qquad\qquad\qquad\qquad (j = 1, 2, ..., n) \\ \dot{y}_j = \alpha_j \left[1 - y_j - \mu\, y_j\, \theta(x_j)\right] \end{cases} \tag{3}$$

where the variable U is the normalised concentration of Li^+ averaged over the n cells considered. In fact, there is certainly a statistical distribution on all the parameters α_j, ρ, β, μ, K around average values. Nevertheless, numerical simulations show that such fluctuations may be reproduced in varying the single control parameter α_j. Indeed, the most relevant characteristic of the local oscillator is the main frequency f_j associated with the limit cycle generated when the jth cell is isolated. A strong dependence of this frequency f_j on the α_j-value is observed (Fig. 4). Oscillators with different frequencies or even without any oscillation ($\alpha_j > 0.26$) may be obtained. The synchronisation and the effect of inactive cells may thus be investigated.

The critical value δ_c of the coupling parameter δ for which synchronisation occurs is estimated to be equal to 0.4 from the experimental data. The critical value

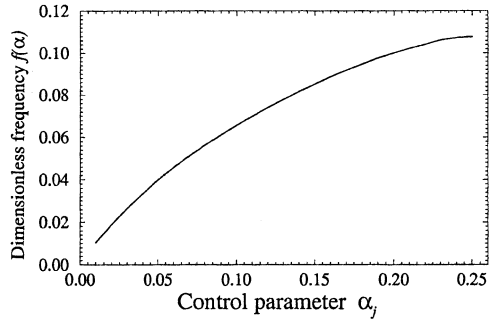

Fig. 4. Dependence of the main frequency of the local oscillator on the α_j-value. The other control parameters are equal to those used in Fig. 3. Thus, varying the values of the parameters α_j is sufficient to reproduce the distribution of periods observed in cells within a skin.

observed from numerical simulations is around 0.1145 when four cells are taken into account (Fig. 5). Obviously, the simplifications which have been applied forbid quantitative simulations, but it has been observed that this value increases with the number of cells used for the simulations. For instance, for $n = 25$, the critical value is approximatively equal to 0.2315. Consequently, increasing the number n of oscillators improves the accuracy of the model. Nevertheless, we observed that the nature of the behaviour is not dependent on that number. Indeed, the synchronisation always occurs according to the same scenario. Only the power spectrum becomes more complicated, but the global behaviour remains a quasi-periodic one, with a dimensionality that mainly depends on the number of significantly different frequences associated with the oscillators. Such a feature results directly from the special form of the coupling between cells. In particular, the fact that the coupling is global and does not result from interactions with nearest neighbours strongly constraints the dynamics. Investigating the nature of synchronisation for a spatially explicit coupling using techniques as reviewed by Pikovsky et al. [12] is postponed for future works. We will thus describe the nature of the synchronisation only using four cells.

In fact, for a given n, such a synchronisation progressively appears when the coupling δ is increased. The evolution of the asymptotic behaviour observed for different values of the coupling constant δ is shown in Fig. 5. When the coupling parameter δ is small, the evolution of the averaged concentration of lithium U seems to be non-periodic (Fig. 5a). Note that in our experiments it is the potential of the whole skin which is measured. Consequently, the variable related to the physical quantity measured is the normalised concentration of Li^+ averaged over the four cells. Variables x_i and y_i ($i = 1, ..., 4$) cannot be simultaneously measured. When the coupling δ is increased, the asymptotic

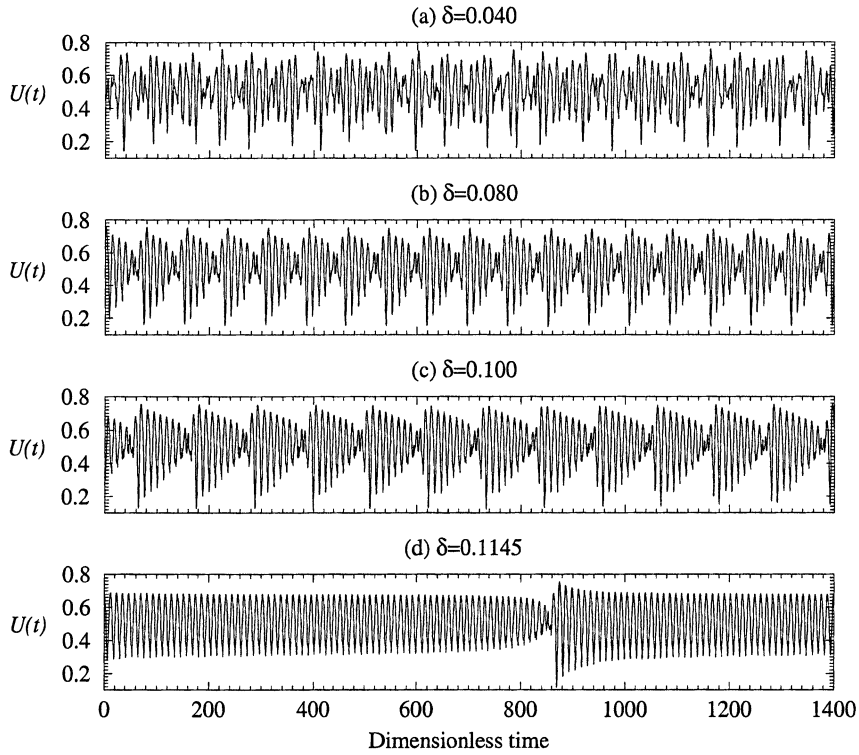

Fig. 5. Progressive synchronisation of the different regions of the epithelium versus the coupling constant δ. Four cells are used with parameter $\alpha_1 = 0.24$, $\alpha_2 = 0.14$, $\alpha_3 = 0.26$ and $\alpha_4 = 0.10$, respectively. The other control parameters are equal to those used in Fig. 3.

behaviour becomes more singular (Fig. 5b and c), and when δ is very close to the critical values δ_c, the behaviour becomes almost periodic during long time intervals (Fig. 5d). Between these so-called *laminar phases*, bursts, during which the amplitude of oscillation fluctuates significantly, are observed (Fig. 5d). When δ is greater than δ_c, no burst is observed anymore and the asymptotic behaviour is periodic, as suggested by the experimental data shown in Fig. 1a. Note that what is relevant is the number of cells with different main frequency f_j. Indeed, if many cells have the same frequency, the critical value δ_c decreases.

In order to characterise the transition from the aperiodic behaviours to the periodic ones, it may be convenient to compute power spectra from the normalised concentrations U of Li^+ averaged over the four cells (Fig. 6). In the power spectra computed for $\delta = 0.040$, three main frequencies are identified (Fig. 6a). Their values are reported in Table 1. It may seen surprising that only three frequencies are identified, since four cells are involved in our simulations. In fact, two α_j values are very close, namely $\alpha_1 = 0.24$ and $\alpha_3 = 0.26$. Moreover, the dependence of the frequency on the α_j-values around 0.25 is very weak (Fig. 4). Consequently, two local oscillators have almost the same eigenfrequency. In the spectrum shown in Fig. 6a, any frequency f_k corresponds to a linear combination between these three frequencies, according to:

$$f_k = n_{1,k}\, f_1 + n_{2,k}\, f_2 + n_{3,k}\, f_3 \qquad (4)$$

where $n_{j,k}$ are integers. Such a spectrum is characteristic of a quasi-periodic motion [13]. In that case, the trajectory visits a torus T^3, which may be embedded in a phase space $\mathbb{R}^4$. To be clear, a torus T^2 embedded in $\mathbb{R}^3$ is the common inner tube. A torus T^n is characterised by n characteristic frequencies and may be embedded in a phase space with a dimension greater or equal to $(n + 1)$.

When the coupling δ is increased, the three frequencies converge around the averaged frequency (Table 1). As a consequence, the power spectrum becomes more regular. When δ is very close to the critical value δ_c, a single frequency is recovered (Fig. 6d), as usually observed for periodic oscillations. It is thus important to characterise how the torus T^3 evolves when δ is increased. The first step is to investigate the dynamics in the phase space.

Since we are mainly concerned with characterising the behaviour of the whole skin, that is, the global behaviour of the n cells, only the averaged concentration U may be used to investigate the underlying dynamics. One of the most interesting results from the

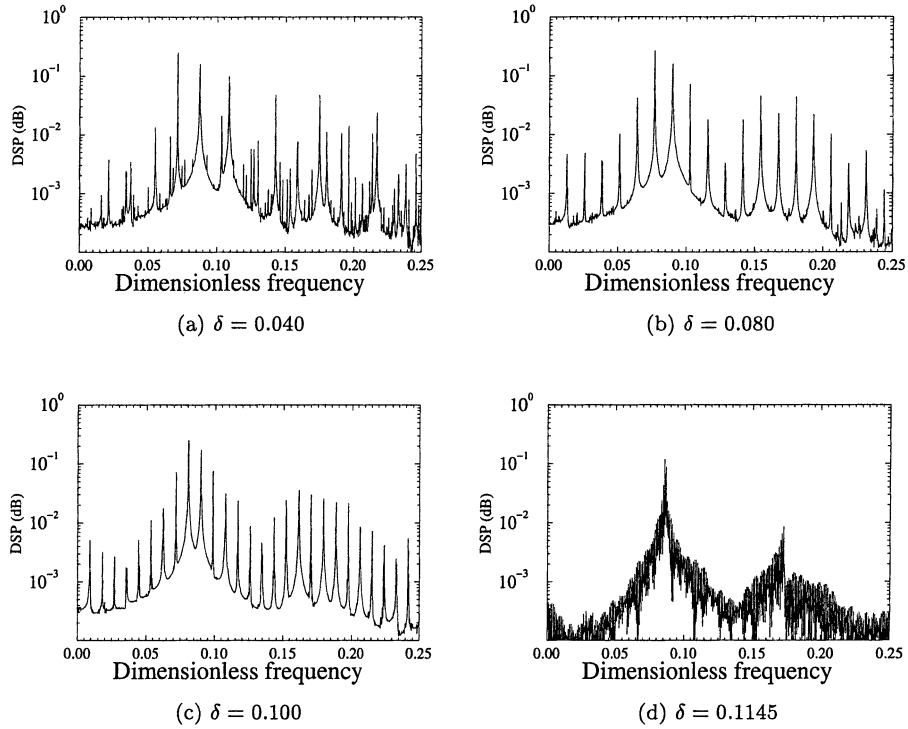

Fig. 6. Power spectra computed from the normalised concentrations $\bar{x}$ of Li^+ averaged over the four cells for different values of the coupling constant δ.

Table 1. Values of the three main frequencies identified in the power spectrum for different values of δ when four cells are involved as in Fig. 5.

δ	f_1	f_2	f_3
0.040	0.072	0.088	0.109
0.080	0.077	0.090	0.103
0.100	0.081	0.090	0.099
0.1145	–	0.086	–

nonlinear dynamical system theory is that it is possible to reconstruct a phase portrait, which is equivalent to the original one, using delay coordinates derived from a single time series [14]. Delay coordinates correspond to a set of independent coordinates derived from $U(t)$, as:

$$\{U(t), U(t+\tau), U(t+2\tau), ..., U(t+(d_E-1)\tau)\} \qquad (5)$$

where d_E is the embedding dimension [15], that is, the minimal number of dynamical variables required for a non-ambiguous description of the states of the system. Such a dimension may be estimated using a false nearest neighbours technique as reviewed by Abarbanel et al. [15] and improved by Cao [16]. In the present case, the embedding dimension is equal to 2 and, consequently, two dynamical variables could be sufficient to reconstruct the phase portrait. In a 2D phase space, according to the Poincaré–Bendixson's theorem, the asymptotic behaviour is necessarily a periodic orbit. In fact, as previously discussed, the behaviour is not exactly periodic and a higher-dimensional phase space is required. The false nearest-neighbours technique fails here because the departure from a periodic behaviour is too small, as discussed below. Note that the embedding dimension does not deal with the correlation dimension of the attractor itself, but with the dimension of the space in which the attractor is embedded. The embedding dimension d_E is therefore an integer. This is a much more interesting quantity than the correlation dimension, since it estimates the number of dynamical variables required for describing the attractor without any ambiguity [17,18]. A correlation dimension d_c may be related to this relevant quantity for practical purpose through the Takens theorem [19], which states that when the dimension d of the space in which the attractor is embedded is greater than $2\,d_c$, we are ensured to have a diffeomorphism between the (unknown) original phase space and the reconstructed phase space. The Takens' criterion does not provide anything for embbeding the attractor in a space with a

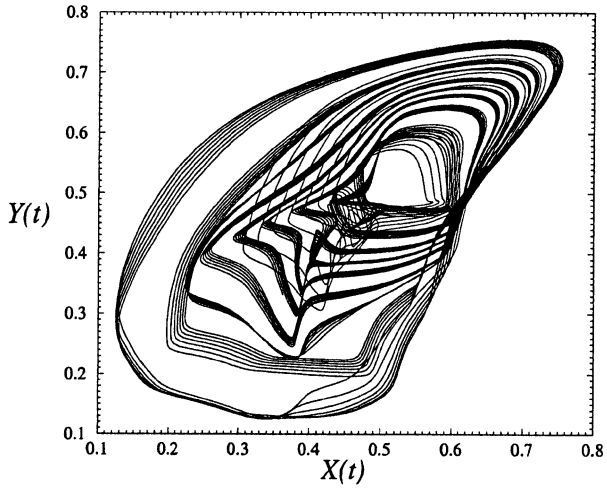

Fig. 7. Phase portrait of the quasi-periodic regime generated by the global model with four cells with a constant δ equal to 0.100. The other control parameters are equal to those used in Fig. 5.

dimension less than $2\,d_c$. This is quite regrettable because, in practice, it is most of the time possible to work in a space with a smaller dimension than $2\,d_c$ [17,18].

A projection of the phase portrait reconstructed from U and spanned by $\{U(t), U(t+\tau)\}$, where the time delay τ is estimated by a visual inspection, is displayed in Fig. 7. Such a visual inspection is guided by the fact that the phase portrait is confined along the first bisecting line when the time delay τ is too small, while it is confined along the second bisecting line and too unfolded when τ is too large [20]. Note that such a phase portrait does not correspond to a chaotic behaviour for which a broad band spectrum is required. The main departure between a chaotic behaviour and a quasi-periodic behaviour is the lack of sensitivity to initial conditions in the latter case.

The second step in a global analysis is to compute a first-return map to a Poincaré section. Roughly, a Poincaré section is the set of the intersections between the trajectory in the phase space with a plane which is never tangent to the trajectory. In the case of the phase portrait displayed in Fig. 7, the Poincaré section is defined by the set

$$P \equiv \{(Y_n, Z_n, W_n) \in \mathbb{R}^3 | X_n = 0.52, \dot{X}_n > 0\} \quad (6)$$

The first-return map is then computed by plotting, for instance, the Y_{n+1}-coordinate of the $(n+1)$th intersection versus the Y_n-coordinate of the nth intersection. For $\delta = 0.1130$, i.e. for a value quite close to the critical value δ_c, the first-return map looks like a closed curve (Fig. 8). In fact, the first-return map is not a closed curve in Fig. 8, but it would be if a much longer time series were used (a full day of computations was already required for Fig. 8). Such a long integration duration is required because the trajectory spends a lot of time in the regions where the first-return map is tangent to the bisecting line. This is why the departure from periodic oscillations is very weak and why the embedding dimension has been found to be equal to 2 (as discussed above). Note that such a closed curve for a first-return map is a signature of a torus that cannot be embedded within a 2D phase space.

In fact, the bifurcation occurs when the first-return map reaches the bisecting line. After that, the trajectory spends an infinite time at the point where the map touches the bisecting line. In that case, $Y_{n+1} = Y_n$ and a periodic orbit is observed. The tangent bifurcation which thus occurs destroys the torus, which is replaced with a stable periodic orbit. The tangent bifurcation is necessarily accompanied with intermittencies between laminar phases during which the behaviour is nearly periodic and bursts associated with significant amplitude fluctuations (Fig. 9). The most often observed intermittencies were introduced by Pomeau and Man-

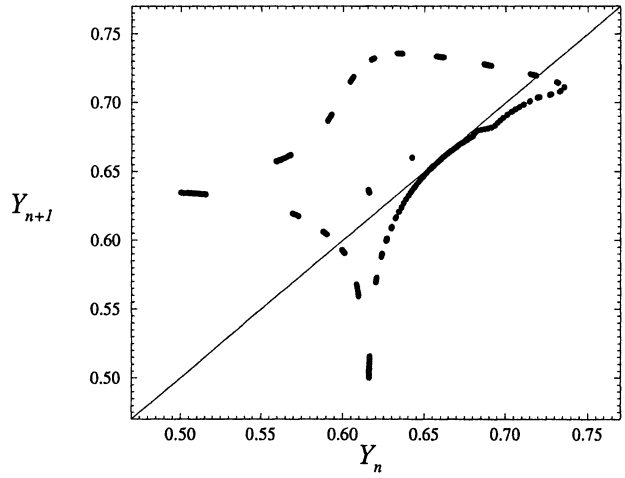

Fig. 8. First-return map to a Poincaré section of the reconstructed phase portrait shown in Fig. 7 for a coupling constant δ equal to 0.113. The other control parameters are those used for Fig. 5.

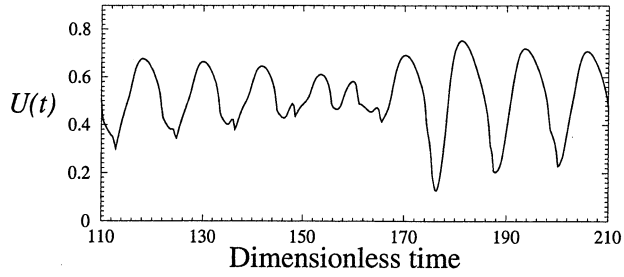

Fig. 9. Amplitude fluctuations during bursts between two laminar phases. Numerical simulations with the four-cell models for $\delta = 0.1145$.

neville [21]. The very interesting feature of these new simulations is that during the bursts, the amplitude evolves significantly as it was observed in experiments (Fig. 1b). Indeed, many experimental observations were done in the early 80's, in which the amplitude of oscillations was constant for a significant time interval and, abruptely, amplitude fluctuations were observed during a relatively short time interval. Such observations were not published by that time since no explanation was available.

5. Conclusion

The model built from an assumption quite simple about the action of the lithium explains, at least qualitatively, different experimental observations. In particular, it allows reproducing the existence of a critical value for the coupling constant beyond which all the cells of the whole skin are synchronised. It describes a situation where the pumping of a charged substance, associated with a non-linear mechanism, allows synchronising a collection of local oscillators without any hormonal action. By using a global analysis in a phase space reconstructed with the delay coordinates, the progressive synchronisation as a function of the coupling constant δ has been identified. It arises through a tangent bifurcation and leads to quasi-periodic behaviours, with amplitude fluctuations which are very characteristic of intermittencies.

Hence, increasing the complexity of the behaviour of the living frog-skin system by inducing electric oscillations via lithium addition to the external solution provided information on this system that could not have been provided by a conventional, reductionist approach. This may be the basis for the introduction of 'complexification', as opposed to reductionism, as a method for studying those properties of a complex system that are destroyed when adopting the conventional, reductive, biochemical approaches.

References

[1] H.H. Ussing, Active and passive transport of the alkali metal ions, Handbuch der experimentellen Pharmakologie, Springer Verlag, Berlin, 1960 pp. 45–143.

[2] C.L. Voute, H.H. Ussing, Some morphological aspects of active sodium transport: the epithelium of the frog skin, J. Cell. Biol. 36 (1968) 625–638.

[3] J. Aceves, D. Erlig, Sodium transport across the isolated epithelium of the frog skin, J. Physiol. 212 (1971) 195–210.

[4] W. Nagel, Influence of lithium upon the intracellular potential of frog skin epithelium, J. Membr. Biol. 37 (1977) 347–359.

[5] S. Takenaka, Studies on the quasiperiodic oscillations of the electrical potential of the frog skin, Jpn. J. Med. Sci. III (1936) 143–197 (Part I) and 198–293 (Part II).

[6] T. Teorell, Rhythmical potential impedance variations in isolated frog skin induced by lithium ions, Acta Physiol. Scand. 31 (1954) 268–284.

[7] M. Thellier, J.-P. Lassalles, T. Seltz, A. Hartmann, A. Ayadi, Oscillations de potentiel et de courant électriques transépithéliaux sous l'effet de lithium, C. R. Acad. Sci. Paris, Ser. D 282 (1976) 2111–2114.

[8] J.-P. Lassales, M. Thellier, C. Hyver, Oscillations de potentiel électrique membranaire sous l'effet du lithium, in: P. Delattre, M. Thellier (Eds.), Actes du colloque *Élaboration et justification des modèles: applications en biologie*, tome II, Maloine, Paris, 1979, pp. 461–495.

[9] J.P. Lassalles, A. Hartmann, M. Thellier, Oscillations of the electrical potential of frog skin under the effect of Li^+: experimental approach, J. Membr. Biol. 56 (1980) 107–119.

[10] J.-P. Lassalles, C. Hyver, M. Thellier, Oscillations of the electrical potential of frog skin under the effect of Li^+: theoretical formulation, Biophys. Chem. 14 (1981) 65–80.

[11] M. Thellier, J.-C. Vincent, S. Alexandre, J.-P. Lassalles, B. Deschrevel, V. Norris, C. Ripoll, Biological processes in organised media, C. R. Biologies (to be published).

[12] A. Pikovsky, M. Rosenblum, J. Kurths, Synchronisation – a universal concept in nonlinear sciences, Cambridge University Press, Cambridge, UK, 2001.

[13] P. Bergé, Y. Pomeau, C. Vidal, L'ordre dans le chaos, Hermann, Paris, 1984.

[14] N.H. Packard, J.P. Crutchfield, J.D. Farmer, R.S. Shaw, Geometry from a time series, Phys. Rev. Lett. 45 (1980) 712–716.

[15] H.D.I. Abarbanel, R. Brown, J.J. Sidorowich, L.S. Tsimring, The analysis of observed chaotic data in physical systems, Rev. Mod. Phys. 65 (1993) 1331–1388.

[16] L. Cao, Practical method for determing the minimum embedding dimension of a scalar time series, Physica D 110 (1997) 43–52.

[17] C. Letellier, J. Maquet, L. Le Sceller, G. Gouesbet, L.-A. Aguirre, On the non-equivalence of observables in phase space reconstructions from recorded time series, J. Phys. A 31 (1998) 7913–7927.

[18] C. Letellier, L.-A. Aguirre, Investigating nonlinear dynamics from time series: the influence of symmetries and the choice of observables, Chaos 12 (2002) 549–558.

[19] F. Takens, Detecting strange attractors in turbulence, in: D.A. Rand, L.S. Young (Eds.), Dynamical systems and turbulence, Warwick 1980, Lect. Notes Math., 898, 1980, pp. 366–381.

[20] T. Buzug, G. Pfister, Optimal delay time and embedding dimension for delay-time coordinates by analysis of the global static and local dynamical behavior of strange attractors, Phys. Rev. A 45 (1992) 7073–7984.

[21] Y. Pomeau, P. Manneville, Intermittent transition to turbulence in dissipative dynamical systems, Commun. Math. Phys. 74 (1980) 189–197.